

Self-catalyst growth of single-crystalline CaB_6 nanostructures

Junqi Xu, Yanming Zhao*, Chunyun Zou, Qiwei Ding

School of Physics, South China University of Technology, Guangzhou 510640, PR China

Received 27 February 2007; received in revised form 1 June 2007; accepted 8 June 2007

Available online 7 July 2007

Abstract

Large-scale calcium hexaboride (CaB_6) nanostructures have been successfully fabricated with self-catalyst method using calcium (Ca) powders and boron trichloride (BCl_3) gas mixed with hydrogen and argon. X-ray diffraction (XRD), scanning electron microscopy (SEM), transmission electron microscopy (TEM), and selected-area electron diffraction (SAED) were used to characterize the compositions, morphologies, and structures of the samples. Our results show that the nanowires are highly single crystals elongated preferentially in the $[1\ 1\ 0]$ direction. The growth mechanism based on the self-catalyst process is simply discussed.

© 2007 Elsevier Inc. All rights reserved.

PACS: D.61.46.+w; 79.70.+q

Keywords: CaB_6 ; RB_6 ; Nanowires; Nanotubes; Nanostructures

1. Introduction

Since the discovery of carbon nanotubes in 1991 [1], one-dimensional (1D) nanomaterials in the form of tubes, wires, and rods have attracted much attention in the past decade because of their interesting geometries, novel properties, and potential applications [2,3]. Many material systems including carbon [1,4,5], semiconductors [2,6,7], oxides [3,8,9], nitrides [10,11], carbides [12,13], and borides [14,15] have been successfully fabricated by a variety of methods. Calcium hexaboride (CaB_6), one of the alkaline earth cubic hexaboride, has been attracting a great deal of attention as a material for structures exposed to high temperatures, for surface protection, and for wear-resistant parts used in a corrosive environment, due to its favorable properties such as high melting point (2373 K), high hardness, chemical stability, and high electrical conductivity [16–18]. It is especially worth noticing that studies have been carried out to determine the feasibility of using CaB_6 and its composites as a potential material for improvement of the abrasion resistance of bricks for converter [19,20].

Therefore, CaB_6 has attracted considerable contemporary interest from both fundamental and practical viewpoint.

Recently, CaB_6 single-crystal nanowires have been synthesized by Xu et al. [15] using the following chemical reaction: $\text{CaO}(\text{s}) + 3\text{B}_2\text{H}_6(\text{g}) = \text{CaB}_6(\text{s}) + \text{H}_2\text{O} + 8\text{H}_2$. However, in the above procedure, B_2H_6 is characterized by both high toxicity and an explosive behavior, which make the whole experiment process dangerous. In addition, the low reaction pressure (~ 155 mTorr) and catalyst (Ni) are also needed, which make the synthesis procedure complicated. The possibility of searching a relatively safe boron source instead of B_2H_6 as original material and using self-catalysts method to synthesize CaB_6 nanostructures at normal pressure are the motivations for this work.

In this article, we report the self-catalyst synthesis of CaB_6 nanostructures by the direct reaction of alkaline-earth metal with BCl_3 and H_2 gas on Si substrates without using Ni as catalyst throughout the whole growth process. Further details about the experiments and discussion will be given in the following sections.

2. Experimental procedure

The CaB_6 nanostructures were synthesized in a conventional tube furnace with a horizontal quartz tube. The reaction

*Corresponding author. Fax: +86 20 8711 2844.

E-mail address: zhaoym@scut.edu.cn (Y. Zhao).

can be expressed as: $\text{Ca(s)} + 6\text{BCL}_3\text{(g)} + 9\text{H}_2\text{(g)} = \text{CaB}_6\text{(s)} + 18\text{HCl(g)}$. The synthetic route can be described as follows. Firstly, high-purity Ca metal powder (commercial 99.9% and with particle size less than 0.05 mm), 0.2 mg in weight, was well dispersed with a thin thickness over a Si substrate (8×8 mm in size). Then the Si substrate with Ca powders on it was loaded in a quartz boat, and the boat was placed in the center of the long quartz tube within a horizontal tube furnace. After the quartz tube was evacuated and filled with nitrogen for three times, the quartz tube was heated under a mixed gas (50% $\text{H}_2 + 50\%$ Ar) flow of about 120 ml/min. When 1000°C was reached, the BCL_3 flow of 30 ml/min was introduced in to the quartz tube and kept for 20 min. Finally, the power was switched off and the furnace cooled to the room temperature under a H_2/Ar flow of 30 ml/min. After cooling, a grey or dark layer was found on the silicon substrate.

The products were characterized and analyzed using X-ray diffractometer with $\text{CuK}\alpha$ radiation, LEO 1530 VP field-emission scanning electron microscopy (SEM) and JEOL JEM-2010 transmission electron microscopy (TEM).

3. Results and discussion

The phase identification of the product was carried out by X-ray powder diffractometer. A step scan mode was adopted with a scanning step of 0.02° and a sampling time of 2 s. Fig. 1 shows the X-ray diffraction (XRD) patterns of the as-prepared CaB_6 product. The XRD patterns of the product were successfully indexed with a cubic lattice using the program Dicvol, and the lattice parameters were further least-squares refined by the program PIRUM as $a = 4.14 \text{ \AA}$ which agrees well with the data from reference (JCPDS card: no. 89-4304). Our XRD analysis results suggest that the as-prepared product is the CaB_6 with cubic phase.

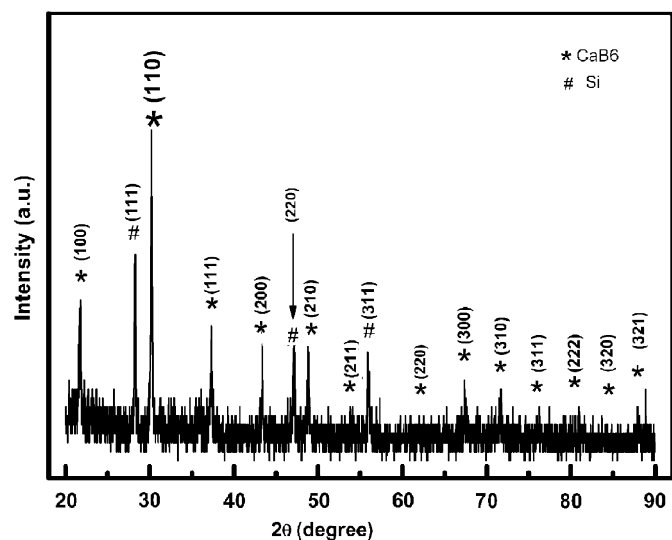


Fig. 1. X-ray diffraction patterns of the sample obtained from Si substrate.

Fig. 2(a) shows a typical SEM image of the synthesized large quantity CaB_6 nanostructures on a silicon substrate. The SEM image (Fig. 2(b)) provides more detail about the morphology of the products. As can be seen from Fig. 2(b), there are two types of morphologies in the CaB_6 structures. One of the morphologies is rectangular shaped plate-like crystals with width of several hundred nanometers, which is the predominant morphology, and the other are nanowires with diameter within 60–100 nm, whose yields are relatively less. Most nanostructures have a smooth surface, and are straight along their axes. No catalyst particles were found on the tips of the nanostructures, which implies that a no catalyst growth process is involved in our experiment.

A typical low-magnification TEM image of the produced CaB_6 nanowires is shown in Fig. 3(a). The nanowire is about 100 nm in lateral dimensions and more than $1 \mu\text{m}$ in length. The nanowire has smooth surfaces and their tips, shown in the low-right inset of Fig. 3(a), are always terminated with a flat surface. Selected-area electron diffraction (SAED) was used to determine the lattice structure of the nanowire. The diffraction pattern appeared identical as we moved the SAED aperture along the entire nanowire, and Fig. 3(d) shows a typical SAED pattern taken along $[1-10]$ zone axis of cubic structure. It reveals

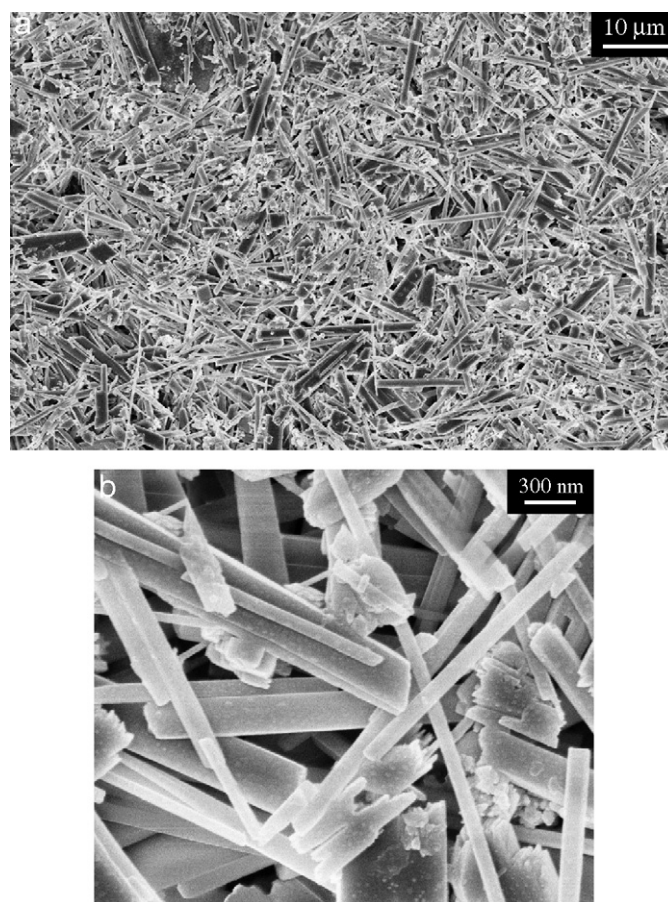


Fig. 2. (a) SEM micrograph of as-synthesized CaB_6 nanostructures. (b) SEM image showing an enlarged view of the CaB_6 nanostructures.

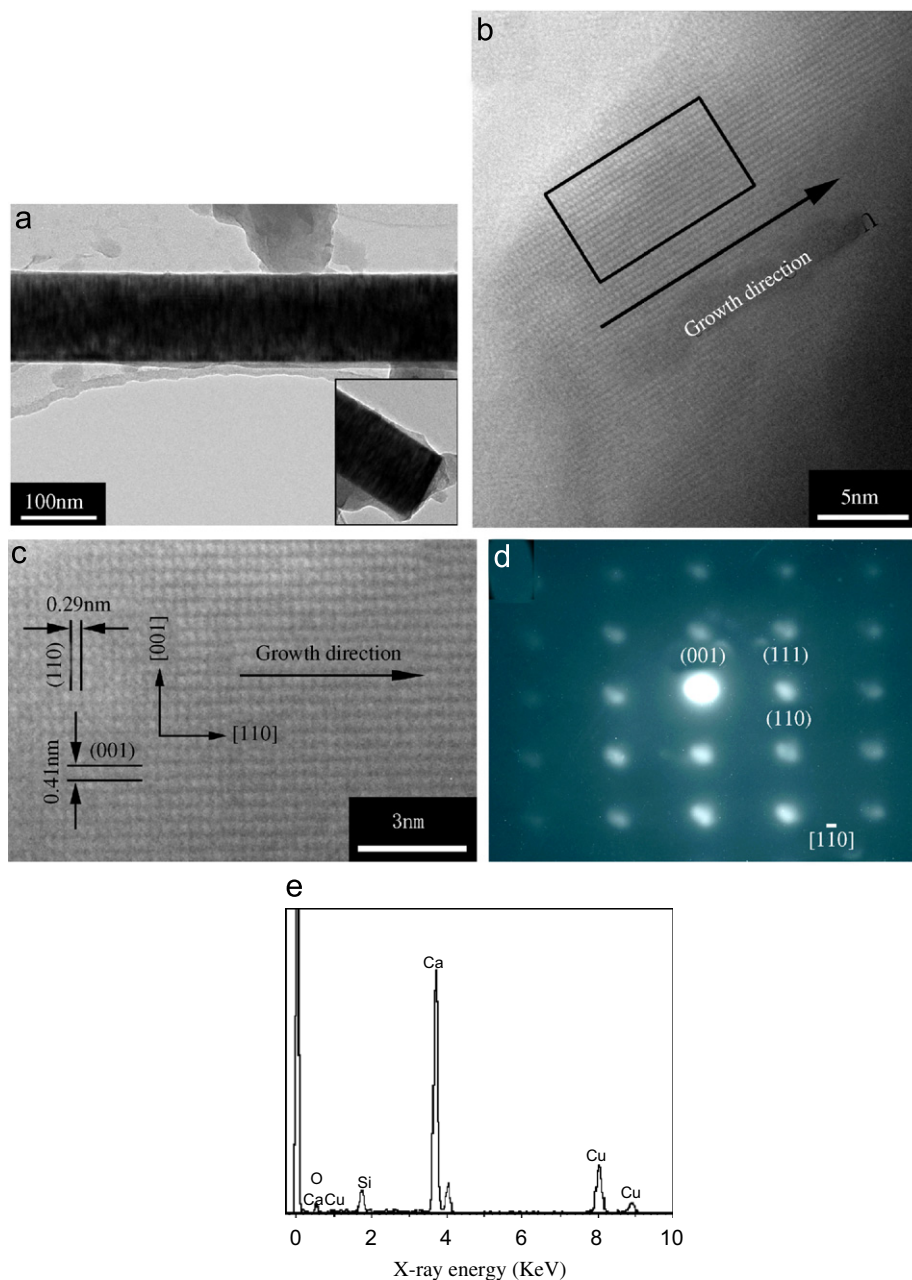


Fig. 3. (a) TEM micrograph of a portion of a nanowire; the insert showing the tip of the nanowire. (b) A representative HRTEM image of the nanowire. (c) HRTEM image of the area of the rectangle in Fig. 3(b) showing a crystallized structure and preferential growth along the $[110]$ direction. (d) The representative SAED pattern recorded along the $[1-10]$ zone axis. (e) EDS spectrum recorded from the nanowire.

that the CaB_6 nanowires adopt single crystal structure which has a primitive cubic structure and the lattice constant a agrees well with our XRD measurement result. To elucidate more details of the atomic structure of the CaB_6 nanowires high-resolution TEM (HRTEM) was also employed. A representative HRTEM image of the nanowire is shown in Fig. 3(b), from which we can see the lattice spacings and an amorphous layer with 5–10 nm thickness surrounding the nanowire. In order to get the clear fringe spacings, the area of the rectangle in Fig. 3(b) was magnified to Fig. 3(c). The lattice spacing of 0.41 and

0.29 nm correspond to the d -spacing of the (001) and (110) crystal faces, respectively. From the HRTEM image, a right angle was formed between the (001) and (110) crystal faces, which is in good agreement with the theoretical value 90.0° . The atom-resolution image also confirms that the nanowire is parallel to the $[110]$ crystallographic direction of the CaB_6 nanowire. EDS technique was also used to study the chemical composition of the catalyst. Fig. 3(e) is a representative EDS spectrum recorded from the nanowire, and the results show that, besides the Ca component, there is little amount of Si, O, Cu in the nanowires.

Because the samples used to analyze the compositions were taken from thin film of nanowires, we think that there may be contamination of our samples with Si substrate (due to etched by BCl_3), especially at the positions that contacted with Si substrate and O (due to the little oxidization of Ca powder before reaction). For the copper composition, it should have come from the Cu grid. It is difficult to detect the B component because of the small atomic number of light elements, and thus based on the analysis of EDS spectrum, it is difficult to confirm the exact compositions of the nanostructures with CaB_6 or not.

One question that needs attention is how the CaB_6 nanostructures grow. The TEM analysis shows that the nanostructures may not be dominated by the conventional vapor–liquid–solid (VLS) mechanism proposed for nanofibres grown by a catalyst-assisted process, in which a transition metal particle is capped at the tip of the fibre and serves as the active catalytic site [21]. We have not observed any metal particles in nanostructures (which would be the evidence for supporting the VLS mechanism) in extensive TEM observations. Here the growth procedure can be described as “self-catalytic” growth [22–24], that is to say, in our experiment, the melting metal Ca plays the role of reactant and catalyst simultaneously. For detailed description of the growth process for the CaB_6 nanostructures, one can refer to our recent work on PrB_6 nanowires, LaB_6 nanowires, and CeB_6 nanowires [22–24].

4. Conclusion

In summary, we have successfully fabricated CaB_6 nanostructures with self-catalysts method using calcium (Ca) powders and boron trichloride (BCl_3) gas mixed with hydrogen and argon. Nanowires, which have diameters in the range 60–100 nm and lengths 1–10 μm , are single-crystalline structure and grow along the [110] axis. Based on the self-catalyst process, a growth mechanism is simply discussed. In addition, we believed this approach, which is based on the simple chemical reaction process and can be readily extended to the synthesis of RB_6 (R = alkaline earth or rare earth) and related boride nanostructures.

Acknowledgments

The authors thank Dan Jiang and Chaolun Liang the Sun Yat-sen University for valuable discussion with the TEM results. This work was supported by the National Nature Science Foundation of China (NSFC, Grants nos.: 50472055).

References

- [1] S. Iijima, *Nature* 354 (1991) 56.
- [2] A. Morales, C.M. Lieber, *Science* 279 (1998) 208.
- [3] Z.W. Pan, Z.R. Dai, Z.L. Wang, *Science* 291 (2001) 1947.
- [4] Z.W. Pan, S.S. Xie, B.H. Chang, C.Y. Wang, L. Lu, W. Liu, W.Y. Zhou, W.Z. Li, L.X. Qian, *Nature* 394 (1998) 631.
- [5] S.S. Fan, M.G. Chapline, N.R. Franklin, T.W. Tombler, A.M. Cassell, H.J. Dai, *Science* 283 (1999) 512.
- [6] X.F. Duan, C.M. Lieber, *Adv. Mater.* 12 (2000) 298.
- [7] Z.W. Pan, Z.R. Dai, L. Xu, S.T. Lee, Z.L. Wang, *J. Phys. Chem. B* 105 (2001) 2507.
- [8] Z.R. Dai, Z.W. Pan, Z.L. Wang, *Adv. Funct. Mater.* 13 (2003) 9.
- [9] Z.W. Pan, S. Dai, D.B. Beach, H.D. Lowndes, *Nano Lett.* 3 (2003) 1279.
- [10] W.Q. Han, S.S. Fan, Q.Q. Li, Y.D. Hu, *Science* 277 (1997) 1287.
- [11] C.C. Chen, C.C. Yeh, C.H. Chen, M.Y. Yu, H.L. Liu, J.J. Wu, K.H. Chen, L.C. Chen, J.Y. Peng, Y.F. Chen, *J. Am. Chem. Soc.* 123 (2001) 2791.
- [12] H.J. Dai, E.W. Wong, Y.Z. Lu, S.S. Fan, C.M. Lieber, *Nature* 375 (1995) 769.
- [13] Z.W. Pan, H.L. Lai, F.C.K. Au, X.F. Duan, W.Y. Zhou, W.S. Shi, N. Wang, C.S. Lee, N.B. Wong, S.T. Lee, *Adv. Mater.* 12 (2000) 1186.
- [14] H. Zhang, Q. Zhang, J. Tang, L.C. Qin, *J. Am. Chem. Soc.* 127 (2005) 2862.
- [15] T.T. Xu, J.G. Zheng, A.W. Nicholls, S. Stankovich, R.D. Piner, R.S. Ruoff, *Nano Lett.* 4 (2004) 2051.
- [16] N. Tsushinsha, in: *Handbook on High-Melting-Point Composites* (Japanese Edition), Nisso Tsushinsha, 1977.
- [17] R.W. Johnson, A.H. Daane, *J. Chem. Phys.* 38 (1963) 425.
- [18] J. Matsushita, S. Komarneni, *J. Mater. Sci.* 34 (1999) 3043.
- [19] S. Hanagiri, T. Harada, S. Aso, S. Fujiwara, H. Yasui, S. Takanaga, H. Takahashi, A. Watanabe, *Taikabutu* 44 (1992) 490.
- [20] S. Hanagiri, S. Fujiwara, H. Kasahara, I. Umehara, H. Yasui, K. Nonobe, H. Takahashi, *Taikabutu* 44 (1992) 640.
- [21] R.S. Wagner, W.C. Ellis, *Appl. Phys. Lett.* 4 (1964) 89.
- [22] J.Q. Xu, X.L. Chen, Y.M. Zhao, C.Y. Zou, Q.W. Ding, *Nanotechnology* 18 (2007) 115621.
- [23] J.Q. Xu, Y.M. Zhao, C.Y. Zou, *Chem. Phys. Lett.* 423 (2006) 138.
- [24] C.Y. Zou, Y.M. Zhao, J.Q. Xu, *J. Cryst. Growth* 291 (2006) 112.